Title Page

Linked structural and functional brain network findings on the biological vulnerability to depression.

Authors: N L Nixon[1], P F Liddle[1], E Nixon[1], G Worwood[1], M Liotti[2], L Palaniyappan[1]

Affiliations: 1. Division of Psychiatry, The Institute of Mental Health, University of Nottingham, Triumph Road, Nottingham, England NG7 2UH. 2. Department of Psychology, Simon Fraser University, Burnaby, BC, Canada.

Declarations of Interest: Dr. N Nixon received funding from the Institute of Mental Health, Nottingham, which enabled him to carry out this research project and has received financial assistance to attend academic meetings from Janssen-Cilag, AstraZeneca, Servier and Shire. Dr. N. Nixon has also taken part in advisory panels for Janssen-Cilag and Servier. Prof. Liddle has received honoraria for academic presentations from Glaxo SmithKline, AstraZeneca, Janssen-Cilag, Bristol Myers Squibb, Eli Lilly and Johnson and Johnson Pharmaceuticals. Prof. Liddle has also taken part in advisory panels for Eli Lilly, Pfizer and Glaxo SmithKline. Dr. E. Nixon reported no biomedical financial interests or potential conflicts of interest. Dr. Worwood has received honoraria for academic presentations from Janssen-Cilag. Dr. M Liotti received a grant from the National Alliance for Research on Schizophrenia and Depression (NARSAD). Dr. Palaniyappan has received a travel fellowship from the International Bipolar Disorder Society sponsored by Eli Lilly in 2010.

Corresponding Author: Dr. N L Nixon, Division of Psychiatry, the Institute of Mental Health, University of Nottingham, Triumph Road, Nottingham, England NG7 2TU, United Kingdom. Email neil.nixon@nottingham.ac.uk

ABSTRACT:

Background: Patients in remission/recovery following episodes of Major Depressive Disorder (MDD) remain highly vulnerable to future relapse/recurrence. Whilst psychological determinants of this risk are well established, little is known about associated biological mechanisms. Recent work has implicated the Default Mode Network (DMN) in this vulnerability but specific hypotheses remain untested within the high-risk, recovered-state of MDD. **Aims:** 1) To test the hypothesis that there is excessive Default Mode Network (DMN) functional connectivity (FC) during task performance within recovered-state MDD; 2) To test for connected DMN cortical gyrification abnormalities. **Method**: A multimodal fMRI/MRI study, including task-based FC and cortical folding analysis, comparing 20 recovered-state MDD patients with 20 matched healthy controls. **Results:** Recovered-state MDD patients showed significant task-based DMN hyperconnectivity, associated with hypogyrification of key DMN regions (bilateral precuneus). **Conclusions:** This is the first evidence of connected structural and functional DMN abnormalities in recovered-state MDD, supporting recent hypotheses on biological-level vulnerability.

INTRODUCTION:

Patients who have recovered from episodes of Major Depressive Disorder (MDD) remain highly vulnerable to future recurrence. Clinical studies put this risk of further MDD episodes at up to 80% (1) in contrast with the general population lifetime risk of 6.7% (2). Whilst psychological determinants of this risk are well established (3, 4), relatively little is known about associated biological mechanisms. Functional Magnetic Resonance Imaging (fMRI) studies have provided some early data on the presence of functional brain abnormalities in recovered-state patients with MDD when performing executive tasks (5, 6). However, there remains no published evidence on brain network functional connectivity (FC) or related structure in recovered MDD despite credible recent hypotheses of their importance. The clearest theory concerns the Default Mode Network (DMN); a brain network in which increased levels of activity have well evidenced associations with internally focused appraisal (7) and which has therefore been considered a potential neural substrate for the ruminative, introspective cognitive patterns of MDD (8-10). The DMN is further implicated through convergent findings of increased resting-state FC between specific DMN regions (namely the dorsomedial Prefrontal Cortex (dmPFC) and precuneus) in both depressed-state MDD (11) and never-depressed, first-degree relatives of patients with recurrent MDD (9); leading the authors of a recent review to hypothesise that DMN hyperconnectivity continues within recovered-state MDD, persisting into task-based activity where it acts as a substrate for overly internal processing, interfering with the recruitment of more effective networks and ultimately creating biological-level vulnerability to depression (10). Recent evidence linking FC and gyrification of the cortical surface (12), means we might additionally predict that abnormal DMN FC is associated with abnormal gyrification in key DMN regions. In light of this literature, our aims were firstly to test the hypothesis that there is excessive task-based DMN FC within recovered-state MDD; and secondly to test the hypothesis that there are connected abnormalities in cortical gyrification within anatomical regions of the DMN.

METHOD:

Recruitment and Clinical assessment:

The recruitment and assessment of this population has been previously reported in detail (5) but is summarised here for convenience.

Patients were recruited through physician referral from general adult psychiatric clinics in Nottingham, UK. Controls were mainly recruited through posters displayed at a General Hospital and a community surgery in Nottingham. Following complete description of the study, written, informed, capacitous consent was obtained from all participants. The study was approved by the Local Research Ethics Committee.

All potential recruits underwent an initial psychiatric assessment by senior clinical psychiatrists (NN, GW, PL), including a detailed history of personal and family psychiatric/medical disorder, substance abuse and medication history; followed by the Structured Clinical Interview for DSM-IV Axis I Disorders (SCID-CV) (13); 2 measures of depressive symptoms, the 17-item Hamilton depression rating scale (Ham-D) (14) and the Beck Depression Inventory – II (BDI-II) (15); 2 measures of personality, the Short Eysenck Personality Questionnaire-revised (EPQ-R) (16) and the Personality Disorders Questionnaire-version 4 (PDQ-4+)(17); a measure of IQ, the Ammons Quick Test (Quick) (18); a measure of cognitive function, the Folstein Mini-Mental State Examination (MMSE)(19); a handedness questionnaire (RIC) (20); and a fMRI safety questionnaire.

A clinical consensus meeting followed initial screening to determine inclusion/exclusion. Minimum inclusion for the patient group required at least 2 previous episodes of DSM-IV Major Depression, diagnosed through SCID-CV, now in recovered-state (with normalized function for at least 3 months and 17-item Ham-D < 8). Exclusion criteria were co-morbid axis I psychiatric disorder (with particular focus on misdiagnosed Bipolar II disorder or anxiety disorders); personality disorder; drug or alcohol disorder; untreated medical disorder; any previous or current CNS disease; or fMRI safety issues. In

addition to the above criteria, potential controls were excluded if there was evidence of any current or past psychiatric disorder.

Patients were followed up over 1 year for evidence of recurrence, determined through use of the SCID-CV at 4-month intervals combined with clinical data from case-notes and treating clinicians.

Statistical testing of clinical, demographic and behavioural data used SPSS 16.0 (http://www.spss.com) and applied the significance criterion $p < 0.05$, with equal variances not assumed. All t-tests were 2-tailed.

Image Acquisition:

BOLD data acquisition: Gradient Echo-Echo Planar Images were acquired using a Philips 3T system during 2 separate 10-minute sessions of a Go/NoGo (GNG) paradigm. Following T2* image stabilisation, 252 volumes of 36 contiguous descending slices were collected (image matrix 64*64, voxel size 3mm*3mm*3mm, field of view 19.2cm, Echo Time 40ms and Repetition Time 2300ms). All subjects received standardized preparation aimed at minimizing performance variance and anxiety (including scripted explanation, practice sessions of the task and habituation within the scanner).

The GNG paradigm has been previously reported in detail (5) but is summarised here. Go (x) or No-Go (k) stimuli were presented on a projected screen for 267ms; inter-stimulus interval was jittered and pseudorandom between 3100–3700 ms, so that each subject had either 159 or 160 stimuli per block of which 32 or 33 were No-Go. Subjects were asked to respond as quickly as possible (by a single button press) when shown the letter ‘x’ and to withhold response when shown the letter ‘k’. The only explicit feedback used during task was the message ‘Too Slow’, shown for correct responses to ‘x’ that were delayed beyond an individually calculated time ceiling, derived from response times in the pre-fMRI practice sessions.

BOLD data Functional Connectivity (FC) analysis:

First-level analysis: PAR/REC format data from the 3T Philips system were converted to NIfTI format using the program dci2nii (http://www.mccauslandcenter.sc.edu/mricro/mricron/dcm2nii) based on MRIcron (http://www.mricron.com). The converted images were then pre-processed using DPARSFA (http://www.restfmri.net) (21) based on REST (http://www.restfmri.net) and SPM8 (http://www.fil.ion.ucl.ac.uk/spm). During pre-processing, images were reoriented, slice timed, spatially realigned, co-registered, segmented, normalised and smoothed to 8mm. The fMRI time series was then subject to linear detrending and temporal bandpass filtering (0.01 – 0.08 Hz) before regressing out motion parameters, global mean signal, white matter signal and cerebrospinal fluid signal (aimed at removing spurious fluctuations not involved in specific regional correlations). Following methodology validated in task-based FC analysis (22, 23), transformed correlation coefficients (z scores) were calculated to generate seed-region based Functional Connectivity z (FCz) maps in DPARSFA, based on 8mm radius seeds in the left and right precuneus (essential regional components of the DMN, with co-ordinates taken from key published literature (11)). Since the co-ordinates were initially published in Talairach space, a conversion was made from Talairach to Montreal Neurological Institute (MNI) space for the current analysis, using tal2mni (24). For each subject FCz maps were generated independently for the left and right DMN seeds, each containing the voxelwise Pearson coefficients of the correlation between the time-series of BOLD variations in the seed region and the rest of the brain.

Second-level analysis: This comprised a main analysis, in which single subject FCz maps were entered into t-tests, using SPM8, to assess whole-brain significance across-group and between-group (Controls vs. Patients); a subsidiary analysis, assessing maintenance-phase medication effects, in which single subject FCz maps were entered into one-factor analyses of variance (ANOVAs) with 3 levels (Unmedicated Patients, Medicated Patients, Controls); and a region of interest (ROI) analysis to enable direct comparison of our findings with key literature. The ROI analysis used a small volume

correction (SVC) within 12mm radius of bilateral dmPFC regions identified by Sheline et al. as uniquely important 'dorsal nexus' areas within depressed-state MDD exhibiting increased resting-state FC to several networks including the DMN (11). All between group tests used age and session as covariates of no interest.

Significance testing: In keeping with Chumbley and Friston 2009 (25), significance testing in our main and ROI analysis incorporates spatial extent, reporting clusters surviving correction at $P_{FDR\text{-}cor}<0.05$. Voxel-level statistics are additionally reported where appropriate at $P_{FWE\text{-}cor}<0.05$ (e.g. in the case of extensive clusters crossing anatomically defined regions). Since cluster-level statistics are not provided in SPM8 ANOVA, this part of the subsidiary analysis reports voxel-level $P_{FWE\text{-}cor}<0.05$.

Reporting of co-ordinates and illustration of clusters: For ease of comparison with existing literature, all coordinates have been reported in Talairach space, following conversion from MNI space using the program mni2tal (24). Significant clusters have been illustrated with Xjview Version 8.11 (http://www.alivelearn.net/xjview).

T1 image Gyrification analysis:

Surface Extraction: Cortical surfaces were reconstructed using FreeSurfer version 5.1.0 (http://surfer.nmr.mgh.harvard.edu). Standard procedures were followed, as described by Dale et al. (26). Pre-processing used Schaer's method (27), an extension of Zilles' gyrification index approach(28), to measure cortical folding patterns for each of the several thousands of vertices across the entire cortical surface. This automated method provides Local Gyrification Indices (LGIs), numerical values assigned in a continuous fashion to each vertex of the reconstructed cortical surface. The LGI of a vertex corresponds to the ratio of the surface area of the folded pial contour ('buried' surface) to the outer contour of the cortex ('visible' surface) included within a sphere of 25mm radius drawn around each vertex, in line with previous studies (26, 28, 29). Thus the LGI value at each vertex reflects the amount of cortex buried in its immediate locality. Schaer's index captures

both the spatial frequency and the amount of curvature of cortical folds in the locality of each vertex.

Statistical analysis examining the spatial distribution of group differences in gyrification: A vertexwise whole brain analysis was performed to localize brain regions showing the most prominent gyrification differences between groups, assessing gyrification on a point-by-point basis across the entire brain. The vertex-wise LGI measurement for each subject was mapped on a common spherical coordinate system (fsaverage). A general linear model controlling for the effect of age and gender was used to compute differences in gyrification between the groups for the right and left hemispheric surfaces, in keeping with published literature (29, 30). The FreeSurfer version 5.1.0 Query Design Estimate Contrast (QDEC) tool was used to generate between-group contrasts. To correct for multiple testing we used a permutation method with 10,000 simulations and identified clusters that survived a type 1 error rate of 5% at a cluster inclusion threshold of p=0.05 (two-tailed). Reported results are corrected for age and gender (including intracranial volume (ICV) as a covariate in the model did not make any important or significant difference to these results).

To test for spatial overlap in the DMN nodes used in our FC analysis (right and left precuneus) and regions showing prominent gyrification defects, we used mri_vol2surf option in FreeSurfer to project these DMN nodes onto the reconstructed average cortical surface (fsaverage), alongside the clusters that emerged as significant in the vertexwise whole brain gyrification analysis.

RESULTS:

Subjects, clinical and behavioural data:

The demographic and clinical data have been previously reported in detail (5) but are summarized here and in Table 1.

Forty-two individuals (20 patients and 22 controls) met the minimum inclusion/exclusion criteria and hence were recruited. Complete T2* images sensitive to BOLD contrast were collected for 20 patients and 20 matched controls (the first 2 control subjects were excluded due to technical difficulties with image acquisition).

Demographic data indicated that the control and patient groups were well matched for age (range: 24 – 63), gender, IQ and laterality. The MDD group showed high recurrence (mean of 4 episodes) but were in stable recovery at the time of data acquisition (mean 13 months).

Table 1. Demographic and Clinical Data shown for Control and Patients Groups (with ranges for numerical data given in brackets).

	Controls	Patients
Mean age	43 (24 – 63)	45 (25 – 63)
Percentage Male Gender	30%	35%
Mean estimated IQ (from QUICK)	108 (98 – 130)	104 (90 – 120)
Baseline mean Ham-D (17-item)	0.3 (0 - 1)	2 (0 – 7)*
BDI - II	1.8 (0 – 6)	8.1 (0 – 19)*
Neuroticism (EPQ-R)	2.9 (0 – 8)	8.9 (3 -12)*
Percent 1st Degree relatives with MDD	5%	70%*
Mean Age at First Episode MDD	N/A	27 (14 – 38)
Mean Episodes of MDD	N/A	4 (2 – 10)
Mean time since remission (months)	N/A	13 (3 - 36)
Percentage taking any antidepressant	0%	70%*
Group total of antidepressant medication	0	19 (0 – 2)**

**Significant difference between patient and control groups, 2-tailed t-tests p<0.05; ** Significant difference both between patient and control groups and also within patient group, with significantly greater amounts of antidepressant medication in the Non-recurrence group (2-tailed t-test p<0.05).*

Behavioural data: Paired across-group t-tests (n=40) showed significantly faster reaction times (RTs) for error commission trials vs. correct response trials ($t = 7.11$, $df = 39$, $p < 0.001$) in keeping with the literature (31, 32); and significant slowing across-group in RTs for correct response trials following error commission ($t = 6.37$, $df = 39$, $p < 0.001$), again in keeping with the literature (33). There were no significant between-group (controls vs. patients) behavioural differences.

Main Task-based Functional Connectivity (FC) analysis (whole-brain level):

Across-group (n=40) findings: As expected positive and negative FC patterns were very similar for the two DMN seed regions in the right and left precuneus (illustrated using results from the right precuneus seed in Figure 1). Thresholded at $t = 5.23$, with clusters surviving $P_{FDR\text{-}cor} < 0.05$ (and voxels surviving voxel-level $P_{FWE\text{-}cor} < 0.05$), regions of significant positive FC included bilateral precuneus and posterior cingulate cortex (BA31); bilateral anterior cingulate cortex (BA 10, 32, 24); bilateral medial prefrontal cortex (BA10); bilateral temporal cortex (BA21); and bilateral posterior parietal cortex (BA40). Regions of significant negative FC included bilateral supplementary motor area (BA6); bilateral inferior orbitofrontal cortex (BA11); bilateral anterior insula; bilateral precentral gyrus (BA9); and bilateral dorsolateral prefrontal cortex (BA10). These results are consistent with the literature (8).

FIGURE 1: Across-group (n=40), whole-brain significant clusters (thresholded at T=5.23, equivalent to voxel-level FWE-corr <0.05) displayed in transverse slice view on a 152 T1 template (xjview), showing significant positive functional connectivity (red, yellow, green) and negative functional connectivity (blue) with the right precuneus (DMN) seed (7, -60, 21). Figures in the legend represent t values; figures adjacent to transverse slices are z values.

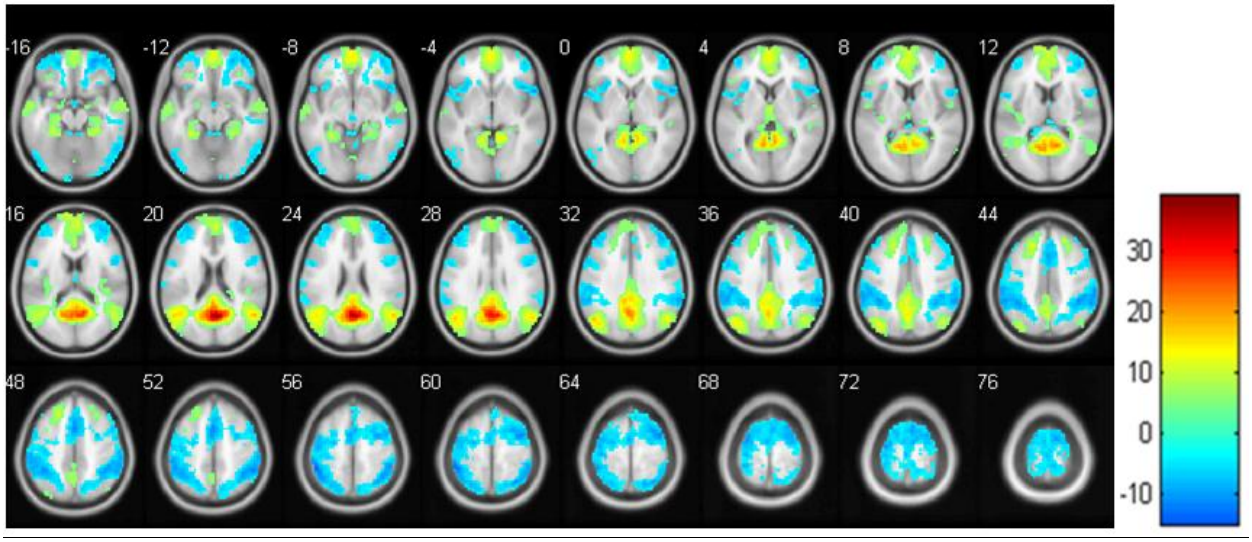

Between-group findings: At corrected whole-brain cluster-level $P_{FDR\text{-}cor}$<0.05 there was significantly greater FC for MDD > Controls from both right and left precuneus seeds to clusters in the right dmPFC (BA9) with some extension into dorsal regions of the right frontal pole (BA10) (statistics given in Table 2). There was also some evidence of increased FC (MDD > controls) to clusters in the left dmPFC (BA9), when thresholded at p <0.001, but this did not survive subsequent whole-brain correction (strongest from the right precuneus seed for MDD > Controls, cluster extent 20 voxels, cluster-level $P_{FDR\text{-}corr}$=0.054 with peak voxel T=4.85 at -24, 34, 43). These findings are illustrated in Figure 2. There were no cluster-level significant findings for controls > patients.

Table 2. Whole-brain significant functional connectivity from Right and Left precuneus (DMN) seeds (+/-7, -60, 21; from Sheline et al. 2010); reporting statistics where whole-brain, cluster-level P survived FDR-corr <0.05.

	Cluster (voxels)	Region (BA)	Cluster-level P (FDR-corr)	Peak T Stat.	Peak Z Stat.	Peak Coordinates (x, y, z)
MDD > Controls						
Right DMN seed						
Right dmPFC	45	9	0.001	4.45	4.18	30, 40, 34
Left DMN seed						
Right dmPFC	27	9	0.025	4.46	4.19	30, 40, 34
	25	10	0.025	4.57	4.28	21, 56, 14
Controls > MDD						
Nil						

FIGURE 2: Rendered images (xjview) of functional connectivity from the left and right precuneus (DMN) seeds for Patients > Controls, thresholded at p <0.001 uncorrected, cluster size > 5 voxels. All right cortical clusters shown here survived subsequent correction at cluster-level $P_{FDR\text{-}cor}$<0.05; left cortical clusters did not survive correction at this level. The superimposed red outline on the right lateral view indicates the most consistent finding of whole-brain significant hyperconnectivity from both left and right precuneus (DMN) seeds to an overlapping area of dmPFC (BA9), also significant within a small volume correction of the right 'dorsal nexus' described by Sheline et al. 2010.

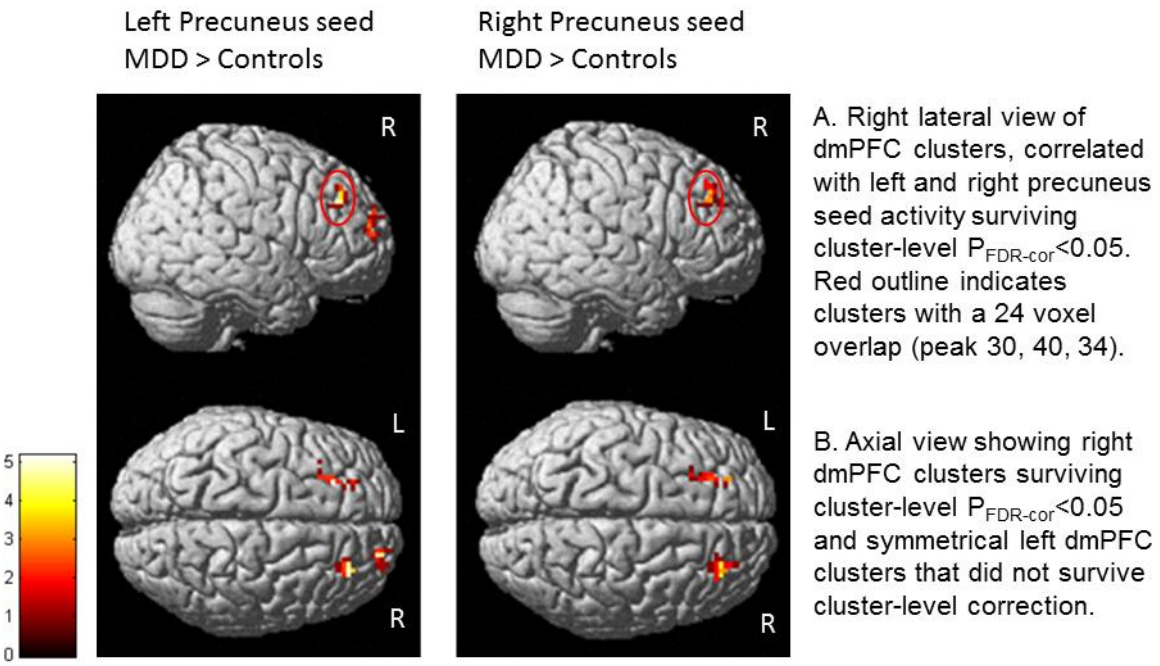

A. Right lateral view of dmPFC clusters, correlated with left and right precuneus seed activity surviving cluster-level $P_{FDR\text{-}cor}$<0.05. Red outline indicates clusters with a 24 voxel overlap (peak 30, 40, 34).

B. Axial view showing right dmPFC clusters surviving cluster-level $P_{FDR\text{-}cor}$<0.05 and symmetrical left dmPFC clusters that did not survive cluster-level correction.

Subsidiary Analysis of Medication Status (Whole-brain level Task-based FC):

Three-group ANOVAs using medicated (n=14), unmedicated (n=6) and control (n=20) groups investigated the effect of continuing maintenance-phase antidepressant medication (detailed in subsidiary material S1) on FC. ANOVA of left precuneus seed FC showed significant main effect of group within a right dmPFC cluster (peak at 30, 36, 39 $F_{2\text{-}75}$ =17.44, $P_{FWE\text{-}corr}$=0.042). Follow-up t-tests, inclusively masked for main effect of group at p<0.001, were significant for Unmedicated patients > Controls at whole-brain level (cluster extent 28 voxels, cluster-level $P_{FDR\text{-}corr}$=0.021, peak T=5.85 at 30, 36, 39). ANOVA of right precuneus seed FC showed main effect that approached significance in the same right dmPFC region (peak at 30, 36, 39 $F_{2\text{-}75}$ =16.60, $P_{FWE\text{-}corr}$=0.075) and given the importance of exploring potential bias through medication follow-up t-tests were performed, masked for main effect of group at p<0.001, showing whole-brain significance for Unmedicated patients > Controls (cluster 33 voxels, cluster-level $P_{FDR\text{-}corr}$=0.006, peak T=5.76 at 30, 36, 39). Figure 3 depicts these main between-group findings, using extracted data from 12mm radius spheres centered on the peak voxel for main effect within the 3-group ANOVAs.

FIGURE 3: Functional connectivity between precuneus (DMN) seeds (Red for Right, Green for Left) and the right dmPFC (30, 36, 39), for unmedicated, medicated and control groups, using extracted data from 12mm radius spheres centered on the peak voxel for main effect within the 3-group ANOVA (with error bars indicating 95% confidence intervals).

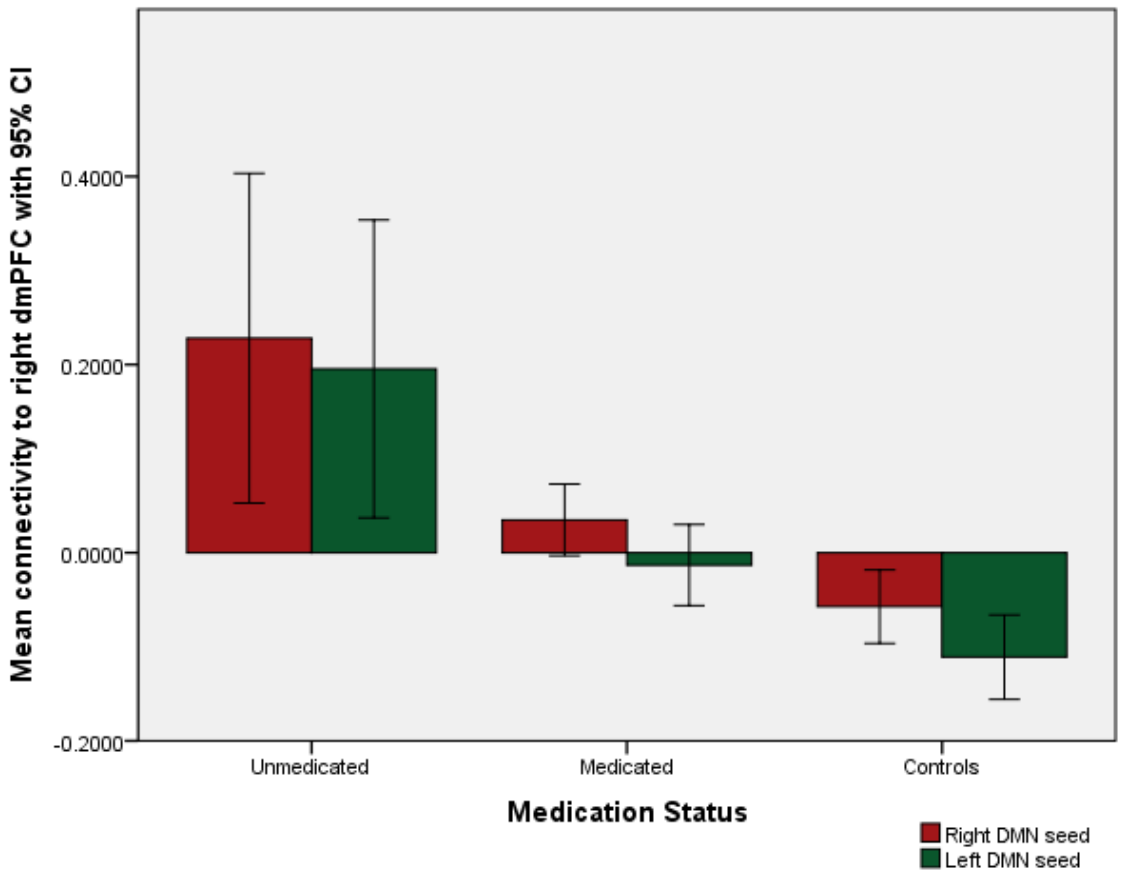

Prospective follow-up of the recovered MDD patient cohort showed that positive medication status was associated with significantly reduced 1-year relapse (RR=0.29, 95% CI 0.10–0.85).

Region of Interest (ROI) Task-based FC analysis:

A separate ROI analysis assessed the proximity of our whole-brain dmPFC findings to specific bilateral dmPFC 'dorsal nexus' regions from the literature (left ROI -24, 35, 28; right ROI 18, 34, 29) (11). Results of this ROI analysis are presented in Table 3, showing significantly increased task-based FC, surviving cluster-level correction $P_{FDR\text{-}cor}<0.05$, between bilateral precuneus regions and clusters within a 12 mm radius sphere centred on the bilateral dmPFC 'dorsal nexus' regions.

Table 3. Showing significant between group functional connectivity differences for bilateral precuneus (DMN) seeds (+/-7, -60, 21; Sheline et al. 2010); reporting clusters surviving FDR-corr <0.05 within 12mm small volume correction of the bilateral dmPFC 'dorsal nexus' regions (Sheline et al. 2010).

	Cluster (voxels)	Region (BA)	Cluster-level P (FDR-corr)	T Stat.	Z Stat.	Coordinates (x, y, z)
MDD > Controls						
Right Precuneus						
Right dmPFC	20	9	0.002	4.10*	3.88	24, 39, 28
Left Precuneus						
Right dmPFC	10	9	0.040	4.04*	3.83	27, 36, 29
Left dmPFC	15	9	0.006	3.70*	3.70	-21, 31, 29
Controls > MDD						
	Nil					

**: Voxel-level significance $P_{FWE\text{-}corr}<0.05$*

Gyrification analysis:

There was significant bilateral hypogyrification (cluster-wise p<0.001, permutation corrected for multiple testing, cluster inclusion threshold p=0.05, n=10,000) in the patient group extending across bilateral medial surface regions incorporating the precuneus. Additionally there was hypergyrification (cluster-wise p<0.001, permutation corrected for multiple testing, cluster inclusion threshold p=0.05, n=10,000) in patients in a more anterior region incorporating the left anterior cingulate cortex. These results are illustrated in figure 4.

To assess the effect of medication in this gyrification analysis we compared medicated and unmedicated patients at the lenient statistical threshold of p=0.10 but did not detect any significant differences. The results of this analysis were unaffected when re-analysed using ICV as an additional covariate.

FIGURE 4: Depiction of whole-brain significant findings from the Gyrification analysis, showing significant (p<0.001) bilateral precuneus hypogyrification (yellow); and hypergyrification (blue) within the left dorsal and rostral anterior cingulate cortex for the patient group compared to controls. Figures in the legend represent T values. The circular Regions of Interest (indicated in red outline) depict the left precuneus DMN seed used in our functional connectivity analysis (taken from Sheline et al.) and a part of Sheline et al.'s 'dorsal nexus'.

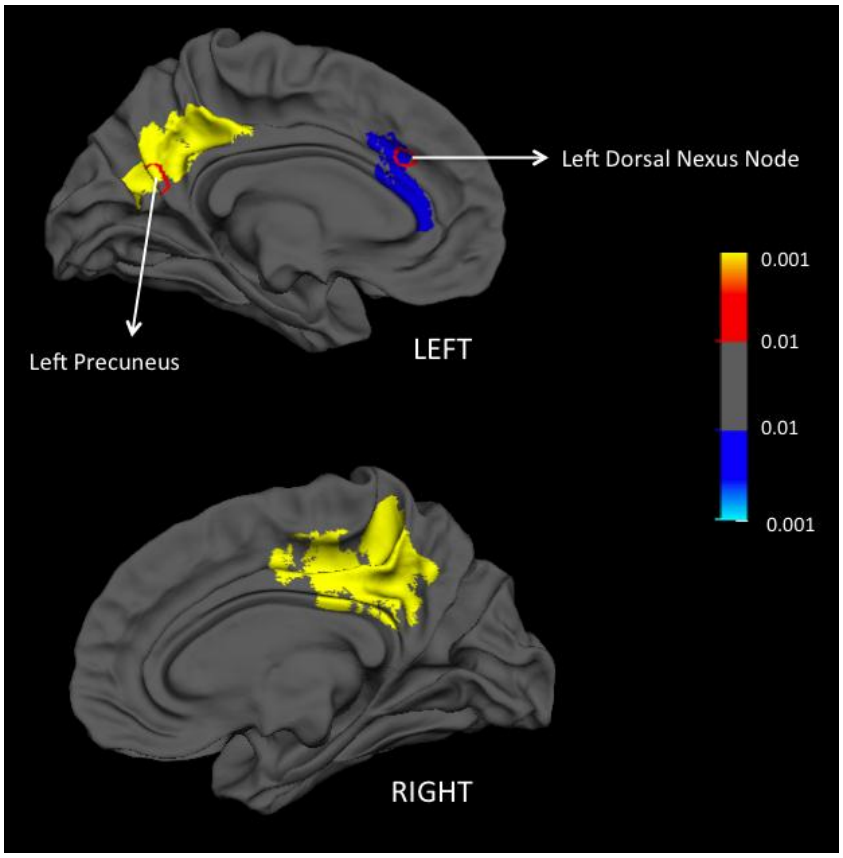

As shown in Figure 4, the left precuneus hypogyrification incorporated the precuneus (DMN) seed used in our FC analysis and originally identified by Sheline et al. (11). Additionally, we mapped Sheline et al.'s left 'dorsal nexus' (-24, 35, 28 spherical ROI of 12mm radius) onto the inflated surface to study the overlap with the gyrification maps. The BA32 part of 'dorsal nexus' (but not the BA8 or BA 9 areas) showed an overlap with the hypergyric ACC cluster identified here. Task-based FC analysis based on this hypergyric ACC cluster (presented in supplementary material S2) identified only one significant finding, of hyperconnectivity for controls > patients within a left posterior tempero-parietal area (cluster 33 voxels, Cluster-level $P_{FDR\text{-}corr}$=0.005, peak T=4.24 at -45, -48, 27).

DISCUSSION:

Our data provide the first direct evidence of task-based DMN hyperconnectivity within recovered-state MDD, confirming a recently published hypothesis (10). This adds to resting-state FC evidence from depressed-state MDD (11) and never-depressed, high vulnerability cohorts (9), supporting the idea that DMN hyperconnectivity is a core feature of the highly recurrent disorder of MDD, extending across different states into apparent clinical recovery. Viewed as a biological substrate, the persistence of DMN hyperconnectivity into recovery is consistent with well-established psychological models that have long identified the persistence of psychological-level risk factors into recovered-state MDD (34). More specifically because of its association with internal focus, DMN hyperconnectivity is a plausible substrate for rumination, observed across states of MDD and described by Beck as involving disproportionate allocation of resources from, 'the external environment to internal experiences' (34). At a brain network level, 'the interference hypothesis' holds that persistence of relatively high DMN connectivity into task interferes with adaptive switching to more appropriate goal oriented brain networks (35). More recently there have been indications that these networks overlap to an unusual degree within MDD (reviewed in (10)) and that the most robustly identified hub in our task-based DMN analysis (right dmPFC, BA9) acts as a 'dorsal nexus', strongly connected to several networks within the depressed-state of MDD (11). Since we have previously shown event-related fMRI hypoactivity within this right 'dorsal nexus' region during active processing (e.g. of error commission) in recovered-state MDD (5), then invoking the 'interference hypothesis' (35) supports the proposition that within recovered-state MDD persistent excessive DMN activity during task, most prominently involving the right 'dorsal nexus', interferes with capacity to appropriately switch this dmPFC (BA9) region to its role in more 'task positive' (active) networks; resulting in cognitive and attentional bias that increases the risk of depression.

The FC findings were associated with bilateral hypogyrification incorporating the precuneus, broadly consistent with the only previous MDD gyrification study that we are aware of, which did not incorporate a FC analysis but demonstrated hypogyrification in a depressed-state MDD cohort extending bilaterally into posterior cingulate/precuneus areas (36). Our data extend this finding by identifying a link between hypogyrification of key DMN hubs (bilateral precuneus) and task-based DMN hyperconnectivity in the recovered MDD group (20 patients vs. 20 controls). In attempting to understand the directionality of this association, we can draw on limited recent evidence from multimodal work in schizophrenia, showing a link between regional hypergyrification and reduced long range FC (12), consistent with the converse finding here of hypogyrification associated with increased long range FC (between the precuneus and dmPFC in the MDD patient group); and also consistent with the FC analysis based on MDD group ACC hypergyrification (associated with relatively reduced long range FC in patients). Since the ACC has been viewed in recent literature as part of a salience network (37), distinct from the DMN, the increased FC in controls between the left ACC and left tempero-parietal regions involved in external cue processing (including speech) could potentially have a functional advantage through enhanced environmental awareness.

Limited evidence from our subsidiary analyses showed no apparent effect of medication status on DMN node gyrification (i.e. significant precuneus hypogyrification was only observed when comparing the whole patient group against controls); but a significant association between medication status and task-based FC, consistent for bilateral precuneus seeds and producing an apparently stratified effect (shown in Figure 3). Whilst we must remain cautious, since one of the groups was small (n=6), the results do at least raise the possibility of a relatively stable structural disruption involving key DMN nodes (observable in significant hypogyrification for the whole patient group vs. controls, without apparent medication status effects), linked to relatively modifiable task-based DMN hyperconnectivity (associated with significant medication status effects). In this case DMN gyrification and connectivity patterns might be thought of as different biological levels of MDD

vulnerability, with the former potentially related to early disruptive effects of trauma on structural aspects of DMN development (8) within the main period of gyrus formation (38).

Limitations: We acknowledge the potential bias introduced by maintenance-phase antidepressant medication in the MDD group. However, additional targeted analyses did not find any association between either task-based FC or gyrification and positive medication status. Indeed, where there was any association with medication status (in task-based FC), this was most abnormal (from both DMN seeds) in patients who had stopped maintenance-phase medication prior to scanning. Although we could not find any indication that maintenance-phase antidepressant medication caused the observed differences in DMN FC or gyrification, we should remain cautious that this part of the analysis (relying on relatively small groups) may have been underpowered to detect real differences.

Additionally, we have presented a seed-region DMN FC analysis using task-based data, following on from extensive literature indicating the validity of this approach, (e.g. (22, 23, 39)), and evidence of persisting, though relatively attenuated DMN activation during a range of tasks, including externally focused activity (39, 40). Although this approach has been shown to provide qualitatively similar results to the analysis of resting-state FC data, caution should be exercised in the quantitative differences that may exist between these approaches (39). This issue is likely to be most problematic when making within-group task-based vs. resting-state FC comparisons and should be much less problematic in the analysis presented here, where we made a between-group comparisons focused purely on task-based DMN FC (i.e. not making experimental comparisons with resting-state). We should also remain conscious of this issue in considering resting-state and task-based studies from the literature; different approaches that often retain mutual relevance, as here (9, 11).

Strengths: We present the first data on DMN connectivity (task-based) in recovered-state MDD and provide the first multimodal analysis relating FC findings in MDD to cortical gyrification. These data test a specific and important hypothesis coming out of the MDD literature.

Implications: Within apparent clinical recovery from MDD there are significant and apparently linked abnormalities in DMN structure (identified through hypogyrification of key hubs) and function (identified through task-based DMN hyperconnectivity). These new findings strengthen our knowledge of the biological-level vulnerability to MDD by confirming and extending an important hypothesis (10) based on previous research (9, 11). When assessed alongside event-related fMRI evidence (5), it seems possible that the identified task-based DMN hyperconnectivity may interfere with switching of important dmPFC areas to more appropriate task-positive activity, in line with earlier theories (35). Further research is needed to confirm the more limited findings that DMN functional hyperconnectivity is greatest in MDD patients who have discontinued maintenance-phase medication; and the theory that this networked brain activity may represent a more dynamic indicator of MDD vulnerability linked to relatively stable cortical gyrification abnormalities.

REFERENCES:

1. Judd LL. The clinical course of unipolar major depressive disorders. Archives of General Psychiatry. 1997;54:989-91.

2. Waraich P, Goldner EM, Somers JM, Hsu L. Prevalence and incidence studies of mood disorders: A systematic review of the literature. Candian Journal of Psychiatry. 2004;49:124-38.

3. Beck AT. Cognitive models of depression. Journal of Cognitive Psychotherapy. 1987;1:5-37.

4. Abramson LY, Metalsky GI, Alloy LB. Hopeless depression: A theory-based subtype of depression. Psychological Review. 1989;96:358-72.

5. Nixon NL, Liddle PF, Worwood G, Liotti M, Nixon E. Prefrontal cortex function in remitted major depressive disorder. Psychological Medicine. 2013;43:1219-30.

6. Norbury R, Selvaraj S, Taylor MJ, Harmer C, Cowen PJ. Increased neural response to fear in patients recovered from depression: a 3T functional magnetic resonance imaging study. Psychological Medicine. 2010;40:425-32.

7. Raichle M, MacLeod MA, Snyder AZ, Powers WJ, Gusnard DA, Shulman GL. A default mode of brain function. Proceedings of the National Academy of Sciences of the United States of America. 2001;98:676-82.

8. Sheline YI, Barch DM, Price JL, Rundle MM, Vaishnavi SN, Snyder AZ, et al. The default mode network and self-referential processes in depression. Proceedings of the National Academy of Sciences of the United States of America. 2009;106:1942-7.

9. Norbury R, Mannie Z, Cowen PJ. Imaging vulnerability for depression. Molecular Psychiatry 2011;16:1067-8.

10. Marchetti I, Koster EHW, Sonuga-Barke EJ, De Raedt R. The default mode network and recurrent depression: A neurobiological model of cognitive risk factors. Neuropsychology Review 2012;22:229-51.

11. Sheline YI, Price JL, Yan Z, Mintun MA. Resting-state functional MRI in depression unmasks increased connectivity between networks via the dorsal nexus. Proceedings of the National Academy of Sciences of the United States of America. 2010;107:11020-5.

12. Dauvermann MR, Mukherjee P, Moorhead WT, Stanfield AC, Fusar-Poli P, Lawrie SM, et al. Relationship between gyrification and functional connectivity of the prefrontal cortex in subjects at high genetic risk of schizophrenia Current Pharmaceutical Design. 2012;18(4):434-42.

13. First MB, Spitzer RL, Gibbon M, Williams JBW. Structured Clinical Interview for DSM-IV Axis I Disorders – Clinician Version (SCID-CV). Washington DC: American Psychiatric Press 1997.

14. Hamilton M. A rating scale for depression. Journal of Neurology Neurosurgery and Psychiatry 1960;23:56-62.

15. Beck AT, Steer RA, Ball R, Ranieri WF. Comparison of Beck Depression Inventories-IA and –II in psychiatric outpatients. Journal of Personality Assessment 1996;67:588-97.

16. Eysenck HJ, Eysenck SBG. Manual of the Eysenck personality scales. London: Hodder and Stoughton; 1991.

17. Hyler SE. Personality Diagnostic Questionnaire (PDQ-4+). New York: New York State Psychiatric Institute; 1994.

18. Ammons RB, Ammons CH. The Quick Test: Provisional manual. Psychological Reports. 1962;11:111-61.

19. Folstein MF, Folstein SE, McHugh PR. 'Mini-mental state'. A practical method for grading the cognitive state of patients for the clinician. Journal of Psychiatric Research. 1975;12:189-98.

20. Oldfield RC. The assessment and analysis of handedness: The Edinburgh inventory. Neuropsychologia. 1971;9:97-113.

21. Yan C, Zang Y. DPARSF: a MATLAB toolbox for "pipeline" data analysis of resting-state fMRI. Frontiers in Systems Neuroscience. 2010;4(13).

22. Rissman J, Gazzaley A, D'Esposito M. Measuring functional connectivity during distinct stages of a cognitive task. NeuroImage. 2004;23:752-63.

23. Hampson M, Driesen N, Skudlarski P, Gore J, RT C. Brain connectivity related to working memory performance. The Journal of Neuroscience. 2006;26:13338-43.

24. Brett M, Christoff K, Cusack R, Lancaster J. Using the Talairach atlas with the MNI template. NeuroImage. 2001;16:abstract 497.

25. Chumbley JR, Friston KJ. False discovery rate revisited: FDR and topological inference using Gaussian random fields. NeuroImage. 2009;44:62-70.

26. Dale AM, Fischl B, Sereno MI. Cortical Surface-Based Analysis: I. Segmentation and Surface Reconstruction. NeuroImage. 1999;9(2):179-94.

27. Schaer M, Cuadra MB, Tamarit L, Lazeyras F, Eliez S, Thiran J-P. A surface-based approach to quantify local cortical gyrification. Transactions on Medical Imaging. 2008;27(2):161-70.

28. Zilles K, Armstrong E, Schleicher A, Kretschmann H-J. The human pattern of gyrification in the cerebral cortex. Anatomy and Embryology. 1988;179(2):173-9.

29. Palaniyappan L, Liddle PF. Aberrant cortical gyrification in schizophrenia: a surface-based morphometry study. Journal of Psychiatry and Neuroscience. 2012;37(1):17-27.

30. Fan Q, Palaniyappan L, Tan L, Wang J, Wang X, Li C, et al. Surface anatomical profile of the cerebral cortex in obsessive–compulsive disorder: a study of cortical thickness, folding and surface area. Psychological Medicine. 2012;Firstview Article:1-11.

31. Ruchsow M, Herrnberger B, Beschoner P, Groon G, Spitzer M, Keifer M. Error processing in major depressive disorder: evidence from event-related potentials. Journal of Psychiatric Research. 2006;40:37-46.

32. Holmes AJ, Pizzagalli DA. Spatio-temporal dynamics of error processing dysfunctions in major depressive disorder. Archives of General Psychiatry. 2008;65:179-88.

33. Laming DRJ. Information theory of choice-reaction times. London: Academic Press; 1968.

34. Beck AT. The evolution of the cognitive model of depression and its neurobiological correlates. American Journal of Psychiatry. 2008;165:969-77.

35. Sonuga-Barke EJ, Castellanos F. Spontaneous attentional fluctuations in impaired states and pathological conditions: A neurobiological hypothesis. Neuroscience and Biobehavioural Reviews. 2007;31:977-86.

36. Zhang Y, Yu C, Zhou Y, Li K, Li C, Jiang T. Decreased gyrification in major depressive disorder. NeuroReport. 2009;20(4):378-80.

37. Sridharan D, Levitin DJ, Menon V. A critical role for the right fronto-insular cortex in switching between central-executive and default-mode networks. Proceedings of the National Academy of Sciences of the United States of America. 2008;105(34):12569-74.

38. White T, Hilgetag CC. Gyrification and neural connectivity in schizophrenia. Development and Psychopathology. 2011;23(1):339-52.

39. Fair D, Schlaggar B, Cohen A, Miezin F, Dosenbach N, Wenger K, et al. A method for using blocked and event-related fMRI data to study "resting state" functional connectivity. NeuroImage. 2007;35:396-405.

40. Duan X, Liao W, Liang D, Lihua Q, Qing G, Liu C, et al. Large-scale Brain Networks in Board Game Experts: Insights from a Domain-Related Task and Task-Free Resting State. Public Library of Science One. 2012;7:1-10.